



product. Acetic acid release results in a decrease in the pH in the local environment (bioactive region) of the enzyme. To monitor the reaction optically, the formation of the proton resulting from enzymatic activity can be followed using an optically measurable signal from an immobilized pH indicator.

Various cholinesterase (ChE) biosensors have been previously developed using different matrices. Wong et al. reported the construction of an optical biosensor based on sol–gel films doped with a lipophilic chromoionophore for the determination of dichlorvos inhibition, an organophosphate insecticide [2]. Moreover, Hai et al. developed a bioelectronic hybrid system for the detection of ACh by immobilizing the AChE enzyme to the gate surface of an anion sensitive field-effect transistor (ISFET) [3]. An amperometric biosensor for the detection of carbamate pesticides based on the inhibition of ACh immobilized by entrapment in an optimized sol–gel matrix on screen-printed electrodes was developed by Bucur et al. [4]. Furthermore, Lenigk et al. presented an electrochemical method for the investigation and comparison of anti-Alzheimer medication based on inhibition of AChE [22].

Liposome-based biosensors have been prepared by encapsulating AChE in L-phosphatidylcholine liposomes resulting in spherical optical biosensors; the enzyme activity within the liposome was monitored using pyranine, a fluorescent pH indicator [8]. Schuvailo et al. developed a carbon fibre-based ACh micro-biosensor for *in vivo* neurotransmitter measurements [9]. A potentiometric AChE biosensor based on a pH-sensitive PVC matrix membrane using a plasma-polymerized ethylenediamine film was prepared by Liu et al. [11] while Choi et al. developed a fiber-optic biosensor consisting of an AChE-immobilized Langmuir–Blodgett film to detect organophosphate compounds in contaminated water [20]. The sensing scheme was based on the decrease of the yellow product, *o*-nitrophenol, from a colourless substrate, *o*-nitrophenylacetate, due to inhibition by organophosphate compounds. In addition to the above mentioned biosensing systems, rapid approaches for preparing sol–gel based fiber-optic biosensors have been developed for both neurotransmitter and insecticide analysis by Doong and Tsai [21] and Xavier et al. [24].

Moreover, donepezil hydrochloride ((±)-2-[(1-benzyl-piperidine-4-yl)ethyl]-5,6-dimethoxyindan-1-one hydrochloride) is a potent, selective and reversible AChE inhibitor that has been prescribed worldwide for the treatment of Alzheimer's disease [28,29]. More recently, donepezil showed potential improvement of Downe's syndrome in a non-randomized controlled trial. In addition, reviews on the pharmacokinetics, pharmacodynamics and clinical profiles of donepezil have been published from which it is apparent that the determination of donepezil in biological fluids has become significant, for which the development of a simple and sensitive method for determining donepezil is required. HPLC methods have been generally reported for determination of donepezil in tablets and plasma [28–32]. Gotti et al. previously described the analysis of donepezil by a capillary electrophoretic method based on the rapid migration of the analyte obtained under acidic conditions [33].

Previous work by the current authors described the synthesis of 2,4-diaryl-5-oxazolone derivatives [34]. This paper concerns the synthesis of three, 5-oxazolone derivatives which contain a phenylazacrown-5 moiety at the 4-position and electron donating and withdrawing groups at the 2-position of the oxazolone. The photophysical characterizations of the fluorescent pH-sensitive CPO-I, CPO-II and CPO-III dyes (Scheme 1) entrapped in PVC matrix were carried out using absorption and fluorescence emission spectroscopies and their application as a biosensing system was investigated. Finally, the newly developed optical biosensors were utilized for both neurotransmitter and inhibitor analyses. The sensor slides were calibrated for donepezil which belongs to a new class of AChE inhibitor as well as the ACh neurotransmitter. Sensor characteristics such as response time, reversibility and repeatability were evaluated.

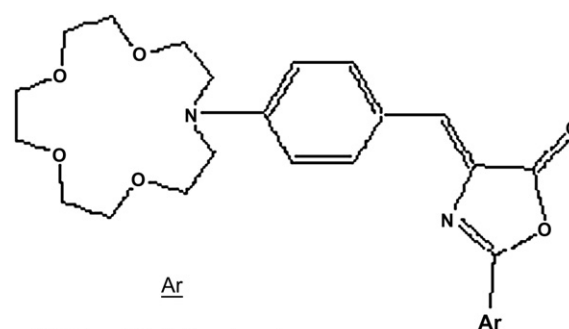
## 2. Experimental

### 2.1. Materials

The CPO-I, CPO-II and CPO-III derivatives were synthesized and purified using the general procedure recounted in Ref. [34]. Acetylcholinesterase (AChE; EC 3.1.1.7, from electric eel, 500 U/mg) and acetylcholine chloride were obtained from Sigma. The membrane components, PVC (high molecular weight) and the plasticizer, bis-(2-ethyl-hexyl)phthalate (DOP), were supplied by Fluka. The lipophilic anionic reagent, potassium tetrakis-(4-chlorophenyl)borate (PTCPB) and tetrahydrofuran (THF) were obtained from Aldrich. All other chemicals were obtained from Fluka and Merck. The Mylar polyester support was provided by DuPont, Switzerland. Bidistilled ultra pure water was used throughout the studies.

### 2.2. Polymer film preparation

The polymer films were prepared from a mixture of 120 mg of PVC, 240 mg of plasticizer, equimolar PTCPB:dye CPO ( $2 \times 10^{-6}$  mol CPO/kg PVC) and 1.5 mL of THF (dry).



CPO-I	3,5-dinitrophenyl
CPO-II	4-nitrophenyl
CPO-III	4-tolyl

Scheme 1.

Finally, AChE (100 unit of AChE in 10  $\mu\text{L}$  of distilled water) was added with stirring and the resulting mixture was spread onto a 125  $\mu\text{m}$  Mylar polyester support. PCV films were kept in a refrigerator at 4  $^{\circ}\text{C}$ . Each sensor PVC film was cut into slides of 12 mm width.

### 2.3. Apparatus and measuring procedures

The absorption spectra of the PVC slides were measured using a Shimadzu UV-1601 spectrophotometer; fluorescence measurements were recorded using a Varian-Cary Eclipse spectrofluorimeter. The pH of buffer solutions was adjusted using a WTW pH-meter calibrated with Merck pH standards of pH 7.00 (titrisol) and pH 4.01. The absorption and fluorescence emission spectra of PVC membranes were obtained using quartz cells which were filled with sample solution. The polymer films were placed in a diagonal position in the quartz cell. The use of this placement method improved the reproducibility of measurements.

AChE was used to catalyze the hydrolysis of ACh (the substrate) to choline and acetic acid. The accompanying reduction in pH of the bulk electrolyte solution was converted to an optically measurable signal by the immobilized dye. The analytical signal corresponds to the rate of decrease in the fluorescence intensity depending on the substrate concentration.

In the case of the AChE inhibitor (donepezil) detection, measurements were carried out in the presence of donepezil and, due to the competitive inhibition of the enzyme, as expected the fluorescence intensity was lowered. These signals were plotted as a function of donepezil concentration. During these experiments, a constant substrate concentration (at saturation level), chosen from the calibration curve of ACh, was used to maintain the enzymes in their active form. Since competitive inhibition occurred, no regeneration step was required before subsequent measurements.

Enzyme–substrate response curves were obtained by using a given amount of ACh substrate in 3 mL of buffer solution. All measurements were performed under ambient conditions and the decrease in fluorescence intensity was recorded with a response time of 4 min.

## 3. Results and discussion

### 3.1. UV–vis absorption and fluorescence emission spectroscopy studies

Absorption and fluorescence emission based photophysical parameters of CPO-I, CPO-II and CPO-III in PVC matrix were extracted from the spectral data and are given in Table 1. The absorption maxima of CPO-I, CPO-II and CPO-III occurred at 488, 509 and 458 nm in PVC film, respectively (Table 1, Fig. 1).

In the PVC matrix, the excitation wavelengths for CPO-I, CPO-II and CPO-III were chosen as 485, 495 and 450 nm, respectively, and emission spectra were recorded (Fig. 2). The CPO dyes exhibited moderate Stokes' shift values, ranging

Table 1

UV–vis absorption and emission spectroscopic data,  $\lambda_{\text{abs}}^{\text{max}}$  (nm),  $\lambda_{\text{emis}}^{\text{max}}$  (nm), Stokes' shift,  $\Delta\lambda$  (nm) and molar extinction coefficients,  $\epsilon_{\text{max}}$  ( $\text{L mol}^{-1} \text{cm}^{-1}$ ) of CPO-I, CPO-II and CPO-III in PVC matrix

CPO	$\lambda_{\text{abs}}^{\text{max}}$	$\lambda_{\text{emis}}^{\text{max}}$	$\Delta\lambda$	$\epsilon_{\text{max}}$
CPO-I	488	590	102	67,000
CPO-II	509	625	116	142,000
CPO-III	458	539	81	175,500

from 81 to 116 nm which confers the advantage of better spectral resolution in emission based studies.

The photostability of the CPO derivatives in PVC was determined with a steady-state spectrofluorimeter in time-based mode. CPO-I, CPO-II and CPO-III were excited at 485, 495 and 450 nm, respectively, and the data were acquired at their maximum emission wavelengths. According to the data collected after 1 h, there was no change in the fluorescence intensities of the sensor slides.

### 3.2. Optimization of biosensor

#### 3.2.1. pH effects on signal intensity

The pH dependence of the sensor systems in the range 6.5–8.2 was investigated both in plain buffers of 2.5 mM phosphate (pH 6.5, 7.0, 7.5, 8.0, 8.2) and in the presence of  $8.33 \times 10^{-5}$  M ACh for CPO-I and CPO-III and  $66.23 \times 10^{-5}$  M ACh for CPO-II substrate containing buffers. The signal change at each pH value was evaluated using the expression  $((I_0 - I)/I_0)100$  in which  $I_0$  represents the fluorescence intensity response of the sensor systems in plain buffers of 2.5 mM phosphate (pH 6.5, 7.0, 7.5, 8.0, 8.2) and  $I$  represents the fluorescence intensity response of the sensor systems in the presence of AChE containing buffers (Fig. 3.). pH 7.0 was chosen as an appropriate measurement medium for CPO-II and CPO-III and pH 7.5 for CPO-I. In order to avoid other interfering pH dependent signal fluctuations, we recorded all of the spectra in phosphate buffered solutions.

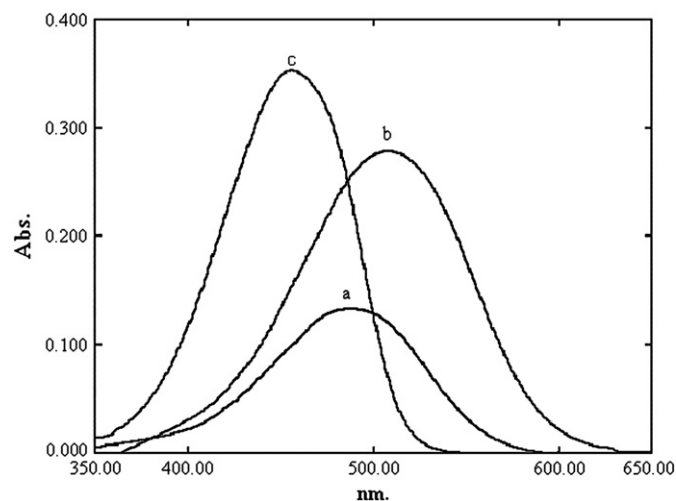


Fig. 1. Absorption spectra of (a) CPO-I ( $\lambda_{\text{max}} = 488$  nm), (b) CPO-II ( $\lambda_{\text{max}} = 509$  nm) and (c) CPO-III ( $\lambda_{\text{max}} = 458$  nm) in PVC ( $2 \times 10^{-6}$  mol CPO/kg PVC, 4 unit AChE activity).

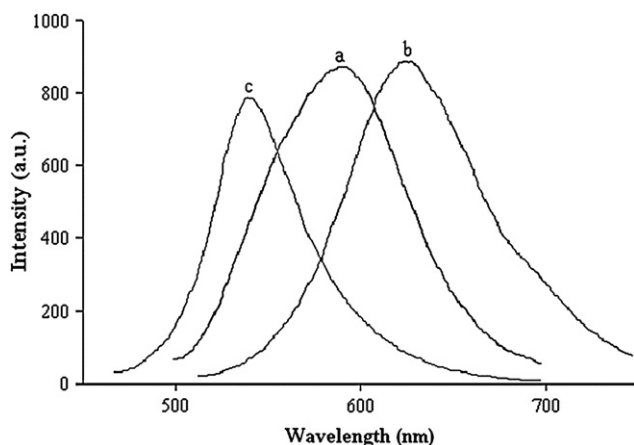


Fig. 2. Emission spectra of (a) CPO-III ( $\lambda_{\max} = 539$  nm), (b) CPO-I ( $\lambda_{\max} = 590$  nm) and (c) CPO-II ( $\lambda_{\max} = 625$  nm) in PVC ( $2 \times 10^{-6}$  mol CPO/kg PVC CPO, 4 unit AChE activity).

### 3.2.2. Response time

The response time of the sensor membrane was investigated in 2.5 mM, pH 7.0 phosphate buffer for CPO-II and CPO-III and at pH 7.5 for CPO-I after the addition of  $8.33 \times 10^{-5}$  M ACh for CPO-I and CPO-III and  $66.23 \times 10^{-5}$  M ACh for CPO-II (Fig. 4). Maximum change in fluorescence intensity due to enzymatic hydrolysis of the substrate was observed after 4 min for all CPO derivatives; this remained constant over time. Thus, the optimum response time of the sensor systems was chosen as 4 min.

### 3.3. Characterization studies

Sensor slides respond to a proton resulting from enzymatic activity. The release of the acid anion decreases the pH of the bulk electrolyte solution which was converted to an optically measurable signal by the immobilized dye. The analytical signal corresponds to the rate of decrease in fluorescence intensity.

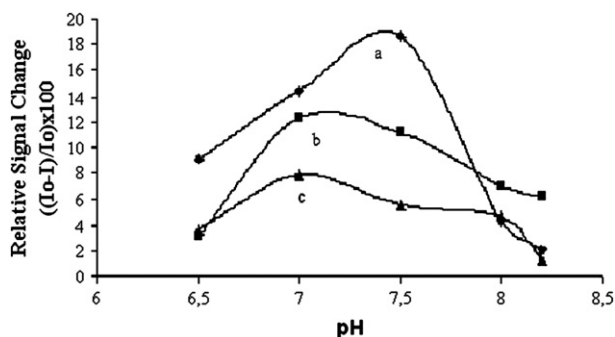


Fig. 3. pH dependence of the fluorescence intensity of (a) CPO-I, (b) CPO-II and (c) CPO-III in PVC ( $2 \times 10^{-6}$  mol CPO/kg PVC, 4 unit AChE activity) in the pH range of 6.5–8.2, in 2.5 mM phosphate buffer;  $I_0$  refers to fluorescence intensity of CPO derivatives in plain buffers of 2.5 mM phosphate and  $I$  refers to buffers containing  $8.33 \times 10^{-5}$  M ACh for CPO-I and CPO-III and  $66.23 \times 10^{-5}$  M ACh for CPO-II.

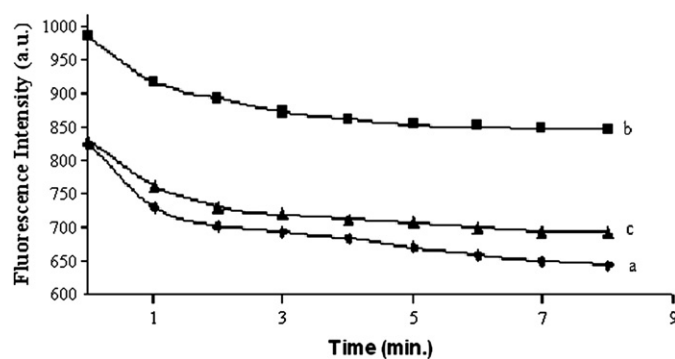


Fig. 4. Fluorescence intensity decrease of (a) CPO-III, (b) CPO-I and (c) CPO-II in PVC ( $2 \times 10^{-6}$  mol CPO/kg PVC, 4 unit AChE activity) in 2.5 mM, pH 7.0 phosphate buffer for CPO-II and CPO-III, and pH 7.5 for CPO-I, after addition of  $8.33 \times 10^{-5}$  M ACh for CPO-I and CPO-III and  $66.23 \times 10^{-5}$  M ACh for CPO-II.

The analytical characteristics of CPO-based biosensing systems in terms of linear range, equation, limit of detection (LOD), etc. for ACh are summarized in Table 2.

The LOD values obtained reveal that the sensitivity of the sensor membranes of CPO-II was approximately 15–19-fold lower than that for the other two. This can be attributed to the electron deficiency of the possible locations of proton attack in the molecules caused by the nitro group located in the *para* position of phenyl.

As shown in Table 2, the linear range of the systems for the ACh substrate was found to be at the sub mM level, which displayed better sensitivity compared to previous work that utilised a fibre optic, based on immobilized AChE and thymol blue biosensor [27] and an optical sensor consisting of a chromoionophore doped sol–gel film interfaced with another sol–gel film immobilized with AChE [2]. An optical system based on ChE/liposome was found to be less sensitive towards to AChE substrate, ATChCl which was at the mM level [8].

#### 3.3.1. Reproducibility and reversibility

The reproducibility and reversibility of the sensor compositions were tested by repeatedly exposing the PVC slides to ACh; the reagent phase was regenerated by 2.5 mM phosphate buffer. The drifts of the upper signal obtained for five cycles and the level of reproducibility achieved are given in Table 3. The RSD values achieved for the response of all three biosensors were very low indicating high reproducibility; the drift

Table 2  
Analytical characteristics of CPO-I, CPO-II and CPO-III based biosensing systems in PVC matrix for ACh

CPO	Linear range (M)	Equation <sup>a</sup>	$R^2$	LOD <sup>b</sup> (M)
CPO-I	$1.67 \times 10^{-5}$ – $33.22 \times 10^{-5}$	$y = 0.0138x + 1$	0.997	$1.01 \times 10^{-5}$
CPO-II	$3.30 \times 10^{-4}$ – $32.26 \times 10^{-4}$	$y = 0.0069x + 1$	0.982	$1.91 \times 10^{-4}$
CPO-III	$1.67 \times 10^{-5}$ – $13.32 \times 10^{-5}$	$y = 0.0118x + 1$	0.992	$1.23 \times 10^{-5}$

<sup>a</sup>  $y$  and  $x$  show fluorescence intensity (a.u.) and concentration (M), respectively.

<sup>b</sup> LOD values were calculated by  $S/N$  ( $n = 3$ ).



Table 3

The drifts of the upper signal obtained for the following five cycles and RSD values of CPO-I, CPO-II and CPO-III in PVC matrix to ACh<sup>a</sup>

CPO	Drifts (%)					RSD (%)
CPO-I	9.2	9.4	9.5	9.7	9.8	0.4
CPO-II	5.5	5.7	6.0	6.5	6.7	0.4
CPO-III	4.9	5.3	5.4	5.6	5.7	0.4

<sup>a</sup> ACh concentrations:  $33.2 \times 10^{-5}$  M,  $32.3 \times 10^{-4}$  M and  $13.32 \times 10^{-5}$  M for CPO-I, CPO-II and CPO-III.

values obtained reveal that the sensor slides were reversible in ACh measurement.

### 3.4. Sensor response for AChE inhibitor: donepezil

As already mentioned, donepezil treatment inhibits enzyme activity and so decreases the fluorescence intensity. Inhibition levels were found to be well correlated with donepezil concentration. Fig. 5 shows the emission spectra of CPO-I in PVC ( $2 \times 10^{-6}$  mol CPO-I/kg PVC, 4 unit AChE activity) in 2.5 mM pH 7.5 phosphate buffer containing  $33.22 \times 10^{-5}$  M ACh in the concentration range of  $7.99$ – $443.86 \times 10^{-7}$  M donepezil.

The reproducibility and reversibility of sensor compositions based on CPO-I were tested by repeatedly exposing the sensor slides to a donepezil concentration of  $443.86 \times 10^{-7}$  M in 2.5 mM pH 7.5 phosphate buffer containing  $33.22 \times 10^{-5}$  M ACh. Each time the reagent phase was regenerated using phosphate buffer at pH 7.0. The relative standard deviation was calculated for the upper signal and was found to be 0.6% for five measurements.

The emission spectra of CPO-II in PVC matrix in 2.5 mM pH 7.0 phosphate buffer containing  $32.26 \times 10^{-4}$  M ACh in

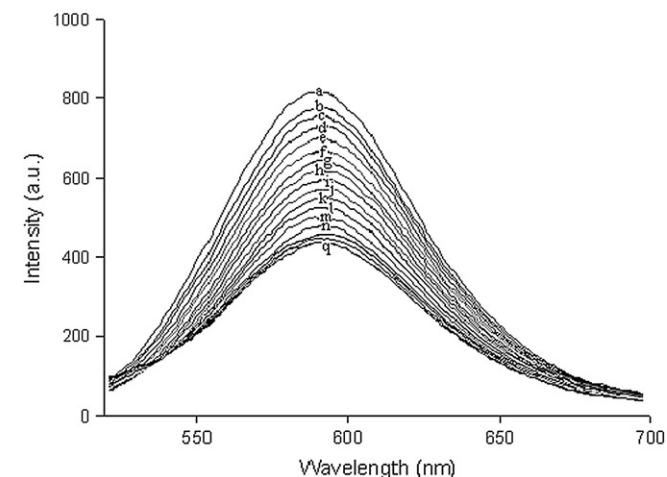


Fig. 5. Emission spectra of CPO-I in PVC ( $2 \times 10^{-6}$  mol CPO-I/kg PVC, 4 unit AChE activity) in 2.5 mM pH 7.5 phosphate buffer containing  $33.22 \times 10^{-5}$  M ACh after exposure to different donepezil concentrations (a) 0, (b) 7.99, (c) 15.99, (d) 31.98, (e) 63.91, (f) 95.81, (g) 127.66, (h) 159.47, (i) 191.24, (j) 222.96, (k) 254.64, (l) 286.28, (m) 317.88, (n) 349.44, (o) 380.95, (p) 412.41 and (q)  $443.86 \times 10^{-7}$  M.

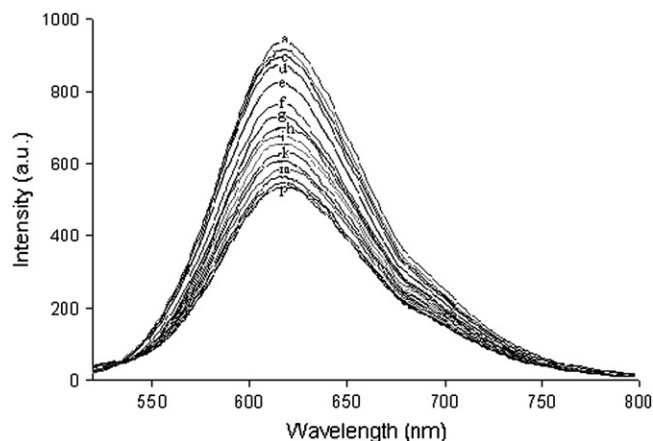


Fig. 6. Emission spectra of CPO-II in PVC ( $2 \times 10^{-6}$  mol CPO-II/kg PVC, 4 unit AChE activity) in 2.5 mM pH 7.0 phosphate buffer containing  $32.26 \times 10^{-4}$  M ACh after exposure to different donepezil concentrations (a) 0, (b) 7.99, (c) 15.99, (d) 31.98, (e) 63.91, (f) 95.81, (g) 127.66, (h) 159.47, (i) 191.24, (j) 222.96, (k) 254.64, (l) 286.28, (m) 317.88, (n) 349.44, (o) 380.95 and (p)  $412.41 \times 10^{-7}$  M.

the concentration range of  $7.99$ – $412.43 \times 10^{-7}$  M donepezil is shown in Fig. 6.

The reproducibility and reversibility of the sensor composition based on CPO-II were determined by repeatedly exposing the sensor slides to a donepezil concentration of  $412.43 \times 10^{-7}$  M in 2.5 mM pH 7.0 phosphate buffer containing  $32.26 \times 10^{-4}$  M ACh. Each time the reagent phase was regenerated using phosphate buffer at pH 7.0. The relative standard deviation was found to be 0.4% for five measurements. Fig. 7 shows the emission spectra of CPO-III in PVC in 2.5 mM pH 7.0 phosphate buffer containing  $13.32 \times 10^{-5}$  M ACh in the concentration range of  $7.99$ – $317.88 \times 10^{-7}$  M donepezil.

In terms of the reproducibility and reversibility of the CPO-III sensor composition, repeated exposure to a donepezil

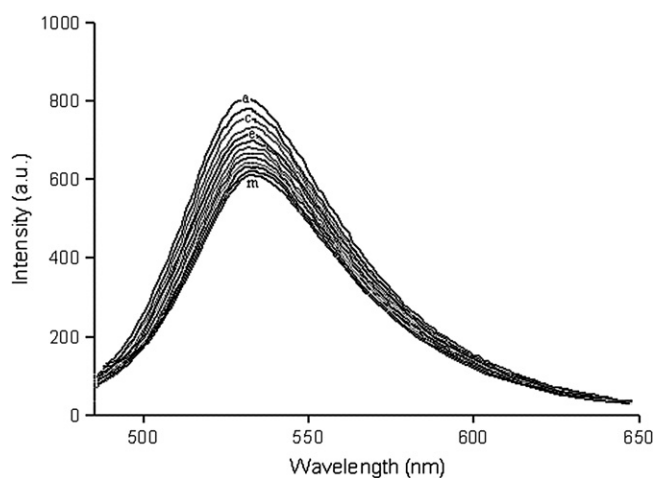


Fig. 7. Emission spectra of CPO-III in PVC ( $2 \times 10^{-6}$  mol CPO-III/kg PVC, 4 unit AChE activity) in 2.5 mM pH 7.0 phosphate buffer containing  $13.32 \times 10^{-5}$  M ACh after exposure to different donepezil concentrations (a) 0, (b) 7.99, (c) 15.99, (d) 31.98, (e) 63.91, (f) 95.81, (g) 127.66, (h) 159.47, (i) 191.24, (j) 222.96, (k) 254.64, (l) 286.28, and (m)  $317.88 \times 10^{-7}$  M.

Table 4

Analytical characteristics of CPO-I, CPO-II and CPO-III in PVC matrix for donepezil (in 2.5 mM pH 7.5 phosphate buffer, ACh:  $33.22 \times 10^{-5}$  M,  $32.26 \times 10^{-4}$  M, and  $13.32 \times 10^{-5}$  M, for CPO-I, CPO-II and CPO-III, respectively)

CPO	Linear range (M)	Equation <sup>a</sup>	R <sup>2</sup>	LOD <sup>b</sup> (M)
CPO-I	$7.99 \times 10^{-7}$ – $443.86 \times 10^{-7}$	$y = 0.002x + 1$	0.990	$3.48 \times 10^{-7}$
CPO-II	$7.99 \times 10^{-7}$ – $412.43 \times 10^{-7}$	$y = 0.0019x + 1$	0.991	$5.02 \times 10^{-7}$
CPO-III	$7.99 \times 10^{-7}$ – $317.88 \times 10^{-7}$	$y = 0.0011x + 1$	0.992	$5.92 \times 10^{-7}$

<sup>a</sup>  $y$  and  $x$  show fluorescence intensity (a.u.) and concentration (M), respectively.

<sup>b</sup> LOD values were calculated by  $S/N$  ( $n = 3$ ).

concentration of  $317.88 \times 10^{-7}$  M in 2.5 mM pH 7.0 phosphate buffer containing  $13.32 \times 10^{-5}$  M ACh and regenerating the reagent phase using phosphate buffer at pH 7.0, revealed that the relative standard deviation was 0.8% for five measurements. Hence, all three sensor systems were fully reversible.

The analytical characteristics of CPO-based biosensing system for donepezil detection are summarized in Table 4.

According to the LOD and RSD values in Table 4, the developed biosensors were sensitive and reproducible to donepezil and there were no considerable differences in the responses of the CPs.

### 3.5. Sensor stability

Sensor stabilities were determined in plain buffers of 2.5 mM phosphate and in the presence of  $8.33 \times 10^{-5}$  M,  $13.16 \times 10^{-4}$  M and  $8.33 \times 10^{-5}$  M ACh containing buffers for CPO-I, CPO-II and CPO-III, respectively. The fluorescence intensity changes as a function of time for the same sensor film over 31 consecutive days of measurements are given in Table 5. The results obtained indicate that the stabilities of the sensor slides were satisfactory.

## 4. Conclusions

Determination of ACh and donepezil was accomplished by the use of newly synthesized CPO-I, CPO-II and CPO-III in plasticized PVC matrices. The sensor membranes were sensitive to ACh in the ranges  $1.67$ – $33.22 \times 10^{-5}$  M,  $3.30$ – $32.26 \times 10^{-4}$  M and  $1.67$ – $13.32 \times 10^{-5}$  M for an average

Table 5

The fluorescence intensity changes vs. time for the same sensor films for CPO-I, CPO-II and CPO-III

Time (days)	Fluorescence intensity					
	CPO-I		CPO-II		CPO-III	
	Plain buffer	ACh containing buffer	Plain buffer	ACh containing buffer	Plain buffer	ACh containing buffer
1	709	675	670	645	763	712
6	705	673	669	643	761	710
11	704	671	665	641	760	706
16	702	670	663	638	757	703
21	698	669	660	634	755	701
26	695	667	658	632	751	695
31	693	663	655	631	748	691

exposure time of 4 min for CPO-I, CPO-II and CPO-III, respectively. The enzyme probes can be used for donepezil sensing in the concentration ranges  $7.99$ – $443.86 \times 10^{-7}$  M,  $7.99$ – $412.43 \times 10^{-7}$  M and  $7.99$ – $317.88 \times 10^{-7}$  M for CPO-I, CPO-II and CPO-III, respectively. The CPO-III sensor membranes were more sensitive to ACh than CPO-I and CPO-II due to electron enrichment of the molecule caused by the *o*-tolyl group. The sensor systems were fully reversible and reproducible, showing that the fluorescent CPO derivatives offer use as alternative indicators for enzymatic neurotransmitter and donepezil sensing.

## Acknowledgements

Funding for this research was provided by the project 2005.KB.FEN.015, Scientific Research Funds of Dokuz Eylul University.

## References

- [1] Dondoi MP, Bucur B, Danet AF, Toader CN, Barthelmebs L, Marty J-L. Organophosphorus insecticides extraction and heterogenous oxidation on column for analysis with an acetylcholinesterase (AChE) biosensor. *Analytica Chimica Acta* 2006;578:162–8.
- [2] Wong FCM, Ahmad M, Heng LY, Peng LB. An optical biosensor for dichlofos using stacked sol–gel films containing acetylcholinesterase and a lipophilic chromoionophore. *Talanta* 2006;69:888–93.
- [3] Hai A, Ben-Haim D, Korbakov N, Cohen A, Shappir J, Oren R, et al. Acetylcholinesterase-ISFET based system for the detection of acetylcholine and acetylcholinesterase inhibitors. *Biosensors and Bioelectronics* 2006;22:605–12.
- [4] Bucur B, Fournier D, Danet A, Marty J-L. Biosensors based on highly sensitive acetylcholinesterases for enhanced carbamate insecticides detection. *Analytica Chimica Acta* 2006;562:115–21.
- [5] Shi M, Xu J, Zhang S, Liu B, Kong J. A mediator-free screen-printed amperometric biosensor for screening of organophosphorus pesticides with flow-injection analysis (FIA) system. *Talanta* 2006;68:1089–95.
- [6] Waibel M, Schulze H, Huber N, Bachmann T. Screen-printed bienzymatic sensor based on sol–gel immobilized *Nippostrongylus brasiliensis* acetylcholinesterase and a cytochrome P450 BM-3 (CYP102-A1) mutant. *Biosensors and Bioelectronics* 2006;21:1132–40.
- [7] Suwanasa-ard S, Kanatharana P, Asawatreratanakul P, Limsakul C, Wongkittisuksa B, Thavarungkul P. Semi disposable reactor biosensor for detecting carbamate pesticides in water. *Biosensors and Bioelectronics* 2005;21:445–54.
- [8] Vamvakaki V, Fournier D, Chaniotakis NA. Fluorescence detection of enzymatic activity within a liposome based nano-biosensor. *Biosensors and Bioelectronics* 2005;21:384–8.
- [9] Schuvailo ON, Dzyadevych SV, El'skaya AV, Gautier-Sauvigne S, Csöregi E, Cespuglio R, et al. Carbon fibre-based microbiosensors for *in vivo* measurements of acetylcholine and choline. *Biosensors and Bioelectronics* 2005;21:87–94.
- [10] Vakurov A, Simpson CE, Daly CL, Gibson TD, Millner PA. Acetylcholinesterase-based biosensor electrodes for organophosphate pesticide detection. II. Immobilization and stabilization of acetylcholinesterase. *Biosensors and Bioelectronics* 2005;20:2324–9.
- [11] Liu B, Yang Y-H, Wu Z-Y, Wang H, Shen G-L, Yu R-Q. A potentiometric acetylcholinesterase biosensor based on plasma-polymerized film. *Sensors and Actuators B* 2005;104:186–90.
- [12] Anitha K, Mohan SV, Reddy SJ. Development of acetylcholinesterase silica sol–gel immobilized biosensor – an application towards oxydemeton methyl detection. *Biosensors and Bioelectronics* 2004;20:848–56.
- [13] Snejdarkova M, Svobodova L, Evtugyn G, Budnikov H, Karyakin A, Nikolelis DP, et al. Acetylcholinesterase sensors based on gold electrodes

- modified with dendrimer and polyaniline A comparative study. *Analytica Chimica Acta* 2004;514:79–88.
- [14] Yadavalli VK, Koh W-G, Lazur GJ, Pishko MV. Microfabricated protein-containing poly(ethylene glycol) hydrogel arrays for biosensing. *Sensors and Actuators B* 2004;97:290–7.
- [15] White BJ, Legako JA, Harmon HJ. Spectrophotometric detection of cholinesterase inhibitors with an integrated acetyl-/butyrylcholinesterase surface. *Sensors and Actuators B* 2003;89:107–11.
- [16] Ricci F, Amine A, Palleschi G, Moscone D. Prussian Blue screen printed biosensors with improved characteristics of long-term lifetime and pH stability. *Biosensors and Bioelectronics* 2003;18:165–74.
- [17] Schulze H, Vorlova S, Villatte F, Bachmann TT, Schmid RD. Design of acetylcholinesterase for biosensor applications. *Biosensors and Bioelectronics* 2003;18:201–9.
- [18] Andreescu S, Barthelmebs L, Marty J-L. Immobilization of acetylcholinesterase on screen-printed electrodes: comparative study between three immobilization methods and applications to the detection of organophosphorus insecticides. *Analytica Chimica Acta* 2002;464:171–80.
- [19] Kok FN, Bozoglu F, Hasirci V. Construction of an acetylcholinesterase – choline oxidase biosensor for aldicarb determination. *Biosensors and Bioelectronics* 2002;17:531–9.
- [20] Choi J-W, Kim Y-K, Lee I-H, Min J, Lee WH. Optical organophosphorus biosensor consisting of acetylcholinesterase/viologen hetero Langmuir–Blodgett film. *Biosensors and Bioelectronics* 2001;16:937–43.
- [21] Doong R-A, Tsai H-C. Immobilization and characterization of sol–gel-encapsulated acetylcholinesterase fiber-optic biosensor. *Analytica Chimica Acta* 2001;434:239–46.
- [22] Lenigk R, Lam E, Lai A, Wang H, Han Y, Carlier P, et al. Enzyme biosensor for studying therapeutics of Alzheimer's disease. *Biosensors and Bioelectronics* 2000;15:541–7.
- [23] Doretta L, Ferrara D, Lora S, Schiavon F, Veronese FM. Acetylcholine biosensor involving entrapment of acetylcholinesterase and poly(ethylene glycol)-modified choline oxidase in a poly(vinyl alcohol) cryogel membrane. *Enzyme and Microbial Technology* 2000;27:279–85.
- [24] Xavier MP, Vallejo B, Marazuela MD, Moreno-Bondi MC, Baldini F, Falai A. Fiber optic monitoring of carbamate pesticides using porous glass with covalently bound chlorophenol red. *Biosensors and Bioelectronics* 2000;14:895–905.
- [25] Choi J-W, Min J, Jung J-W, Rhee H-W, Lee WH. Fiber-optic biosensor for the detection of organophosphorus compounds using AChE-immobilized viologen LB films. *Thin Solid Films* 1998;327–329:676–80.
- [26] Larsson N, Ruzgas T, Gorton L, Kokaia M, Kissinger P, Csöregi E. Design and development of an amperometric biosensor for acetylcholine determination in brain microdialysates. *Electrochimica Acta* 1998;43:3541–54.
- [27] Andreas RT, Narayanaswamy R. Fibre-optic pesticide biosensor based on covalently immobilized acetylcholinesterase and thymol blue. *Talanta* 1997;44:1335–52.
- [28] Nakashima K, Itoh K, Kono M, Nakashima MN, Wada M. Determination of donepezil hydrochloride in human and rat plasma, blood and brain microdialysates by HPLC with a short C<sub>30</sub> column. *Journal of Pharmaceutical and Biomedical Analysis* 2006;41:201–6.
- [29] Radwan MA, Abdine HH, Al-Quadeb BT, Abboul-Enein HY, Nakashima K. Stereoselective HPLC assay of donepezil enantiomers with UV detection and its application to pharmacokinetics in rats. *Journal of Chromatography B* 2006;830:114–9.
- [30] Beglinger LJ, Gaydos B, Tangphao-Daniels O, Duff K, Kareken DA, Crawford J, et al. Practice effects and the use of alternate forms in serial neuropsychological testing. *Archives of Clinical Neuropsychology* 2005;20:517–29.
- [31] Pappa H, Farru R, Vilanova PO, Palacios M, Pizzorno MT. A new HPLC method to determine Donepezil hydrochloride in tablets. *Journal of Pharmaceutical and Biomedical Analysis* 2002;27:177–82.
- [32] Andrisano V, Bartolini M, Gotti R, Cavrini V, Felix G. Determination of inhibitors' potency (IC<sub>50</sub>) by a direct high-performance liquid chromatographic method on an immobilized acetylcholinesterase column. *Journal of Chromatography B* 2001;753:375–83.
- [33] Gotti R, Cavrini V, Pomponio R, Andrisano V. Analysis and enantioresolution of donepezil by capillary electrophoresis. *Journal of Pharmaceutical and Biomedical Analysis* 2001;24:863–70.
- [34] Icli S, Icil H, Alp S, Koc H, McKillop A. NMR, absorption and fluorescence parameters of azlactones. *Spectroscopy Letters* 1994;27(9):1115–28.